Far-infrared magnetic-field-dependent resonances
in small unsupported bismuth particles

R. E. Sherriff and R. P. Devaty

Department of Physics and Astronomy, University of Pittsburgh, 100 Allen Hall, Pittsburgh, Pennsylvania 15260

(Received 7 August 1989)

Far-infrared (5–65 cm^{-1}) magnetic-field-dependent resonances have been observed in free-standing ~0.5-μm-diam bismuth particles prepared by inert-gas evaporation. The number of resonances, the effective masses, and the field dependence of the resonance frequencies differ from bulk Bi. A model based on the quasistatic approximation is developed. The model makes use of the semiclassical complex dielectric tensor with the measured effective-mass tensors and other parameters of bulk Bi. No parameters are adjusted. The success of the model leads to the following interpretation of the data: (1) Both electric- and magnetic-dipole resonances are observed. (2) The particles are not uniformly oriented, since particles with each of the three crystallographic axes (binary, bisectrix, and trigonal) oriented parallel to the applied magnetic field are required to explain the data. (3) The properties of ~0.5-μm-diam Bi particles are bulklike.

I. INTRODUCTION

The semimetal bismuth is an important model system for the study of solid-state plasmas in metals.[1-3] Due to the low density of carriers, the characteristic energies (Fermi energy, energy gap, plasma energy $\hbar\omega_p$,...) are small and of comparable magnitude. Magneto-optical spectroscopy is an effective technique to characterize the anisotropic electronic properties.[4-20] Many types of intraband and interband transitions are accessible using magnetic fields that are routinely achieved in the laboratory. Bi is a unique metal for far-infrared transmission studies because the electrons can be easily driven into the extreme quantum limit.[7]

This paper reports on far-infrared (FIR) magneto-optical absorption by small (~0.5 μm mean diameter) Bi particles. The problem of the interaction of electromagnetic radiation with a small sphere in a magnetic field (the gyrotropic sphere) has attracted recent interest.[21] Applications include the microwave properties of powdered semiconductors[22,23] and the electrodynamic properties of electron-hole droplets.[24] Bi particles have important advantages as a model system. There is less uncertainty in the carrier density relative to semiconductors because doping is not required. The size of the particles can be controlled. Bi particles should not deform much in a magnetic field. Also, the properties of bulk Bi are well known and available as input to models.

The Bi particles are in the form of a free-standing smoke. The high concentration of particles leads to large absorption, which limits the spectral range for transmission to 5–65 cm^{-1}. This is the region of *intra*band behavior. The observed hybrid resonances are analogous to cyclotron resonances.

A semiclassical model based on the quasistatic approximation is developed. When the measured parameters of bulk Bi are used, the predicted behavior for small particles is in agreement with the data. The success of the model leads to the following conclusions: (1) Both electric- and magnetic-dipole resonances are observed. (2) The particles are essentially randomly oriented, since particles with each of the three crystallographic axes oriented parallel to the applied magnetic field are required to explain the data. (3) The properties of ~0.5-μm-diam Bi particles in the very far infrared are bulklike.

In Sec. II we present the model. In Sec. III we discuss sample preparation and characterization. In Sec. IV we present the data and the comparison with the model that leads to the conclusions summarized above. In Sec. V we conclude with suggestions of possible directions for further research on this unique system.

II. MODEL

A. Bismuth dielectric tensor

The frequency-dependent complex dielectric tensor for bulk Bi is obtained from the semiclassical equations of motion.[25,26] A Boltzmann-equation treatment is avoided by assuming that the carrier relaxation times are independent of frequency and the applied magnetic field. The result describes the intraband processes that are of interest in the frequency range covered by the experiments. Quantum effects such as band nonparabolicity, spin-dependent transitions, and magnetic field dependence of the carrier density are neglected.

Undoped Bi has equal densities of electrons and holes distributed in three electron ellipsoids (called A, B, and C) at the L points of the Brillouin zone and a single hole pocket at the T point. The frequency-dependent Drude complex conductivity tensor for the ith carrier type is[25]

$$\tilde{\sigma}_i(\omega) = q_i^2 n_i \left[-i\tilde{\omega}\,\tilde{m}_i + \frac{q_i}{c}H_0\times\tilde{I} \right]^{-1}, \quad (1)$$

where $\tilde{m}_i$ is the effective-mass tensor, $\tilde{\omega} \equiv \omega + i/\tau$ the complex frequency, n_i the number density of carriers, and q_i the charge. H_0 is the applied static magnetic field and $\tilde{I}$ is the identity matrix.

Assuming that the responses of the four types of carriers to an electromagnetic wave can be treated as independent parallel processes, the conductivity tensor for Bi is

$$\tilde{\sigma}(\omega) = \tilde{\sigma}_h + \tilde{\sigma}_A + \tilde{\sigma}_B + \tilde{\sigma}_C . \tag{2}$$

The dielectric tensor is

$$\tilde{\epsilon}(\omega) = \tilde{\epsilon}_L + \frac{4\pi i}{\omega} \tilde{\sigma}(\omega) , \tag{3}$$

where $\tilde{\epsilon}_L$ is the static dielectric tensor due to core polarizability.

The values for the effective mass tensors and $\tilde{\epsilon}_L$ are given by Takano and Kawamura[27] and by Blewitt and Sievers.[7] The densities of carriers were chosen as $n_h = 3.0 \times 10^{17}$ cm^{-3} and $n_A = n_B = n_C = 1.0 \times 10^{17}$ cm^{-3}.

B. Absorption coefficient

The interaction of an electromagnetic wave with the multicomponent anisotropic spherical plasma in a Bi particle has not been solved. The general solution of Ford and Werner[28] (FW) for the gyrotropic sphere does not apply to Bi due to its anisotropy.

In the long-wavelength region of interest here, one can calculate the absorption coefficient using a quasistatic approximation. The FIR properties of an isolated isotropic small metal particle in the absence of an applied magnetic field are described by the long-wavelength expansions of the electric- and magnetic-dipole terms of the Mie solution.[29] For the gyrotropic sphere care must be taken. An expression can be obtained for electric-dipole (ED) absorption, but the electric-quadrupole term must be included with the magnetic-dipole term to obtain correct resonance frequencies and absorption strengths.[21,23,28] There are also magnetic-dipole–electric-quadrupole (MDEQ) cross terms in the FW theory. The correct long-wavelength expressions for the MDEQ extinction have recently been obtained from the FW theory.[21] Since they do not apply to Bi, use is made here of a quasistatic approximation that treats the magnetic-dipole (MD) term alone, which is not rigorously correct. Examination of the correct expressions[21] suggests that the error is small if ϵ_L is much larger than the dielectric constant of the medium surrounding the particles. This is indeed the case for Bi.

There are many approaches to obtain expressions for ED and MD absorption by a small gyrotropic sphere in the long-wavelength limit. The methods chosen here do not require the use of vector spherical harmonics.[30]

1. Electric-dipole term

For generality, consider a uniform isolated ellipsoidal particle with semiaxes a, b, and c and complex dielectric tensor $\tilde{\epsilon}(\omega)$ embedded in a nonabsorbing isotropic dielectric host with real dielectric constant ϵ_0. In the quasistat-

ic limit the derivation is based on electrostatics. Let $\mathbf{E}^{(e)}$ be the uniform external applied electric field and $\mathbf{E}^{(i)}$ the uniform electric field inside the particle. The fields are related according to[31]

$$\epsilon_0 \mathbf{E}^{(i)} + \tilde{L} \cdot (\mathbf{D}^{(i)} - \epsilon_0 \mathbf{E}^{(i)}) = \epsilon_0 \mathbf{E}^{(e)} , \tag{4}$$

where the electric displacement is $\mathbf{D}^{(i)} = \tilde{\epsilon} \cdot \mathbf{E}^{(i)}$ and $\tilde{L}$ is the depolarizing tensor. For spherical particles $\tilde{L} = \frac{1}{3}\tilde{I}$. The explicit relationship between the fields is

$$\mathbf{E}^{(i)} = [\tilde{I} + \tilde{L} \cdot (\tilde{\epsilon} - \epsilon_0 \tilde{I})/\epsilon_0]^{-1} \cdot \mathbf{E}^{(e)} . \tag{5}$$

The particle is polarized by the oscillating applied electric field. The induced dipole interacts with the applied field to produce absorption. For a particle embedded in a nonabsorbing host, only the excess polarization over that of the host leads to absorption. To take this idea into account, define an effective field[32] $\mathbf{P}$ according to

$$\mathbf{D}^{(i)} = \tilde{\epsilon} \cdot \mathbf{E}^{(i)} = \epsilon_0 \mathbf{E}^{(i)} + 4\pi \mathbf{P} . \tag{6}$$

After rearrangement, Eq. (6) becomes

$$\mathbf{P} = \frac{1}{4\pi}(\tilde{\epsilon} - \epsilon_0 \tilde{I}) \cdot \mathbf{E}^{(i)} . \tag{7}$$

The relationship between $\mathbf{P}$ and $\mathbf{E}^{(e)}$, obtained by substituting Eq. (5) into Eq. (7), is

$$\mathbf{P} = \frac{\epsilon_0}{4\pi}(\tilde{\epsilon} - \epsilon_0 \tilde{I}) \cdot [\epsilon_0 \tilde{I} + \tilde{L} \cdot (\tilde{\epsilon} - \epsilon_0 \tilde{I})]^{-1} \cdot \mathbf{E}^{(e)} . \tag{8}$$

As an alternate approach, combine Eqs. (4) and (6) to obtain

$$\mathbf{E}^{(i)} = \mathbf{E}^{(e)} - 4\pi \tilde{L} \cdot \mathbf{P}/\epsilon_0 . \tag{9}$$

Equation (9) is substituted into Eq. (7) to obtain

$$\mathbf{P} = \frac{\epsilon_0}{4\pi}(\tilde{\epsilon} - \epsilon_0 \tilde{I}) \cdot [\epsilon_0 \mathbf{E}^{(e)} - 4\pi \tilde{L} \cdot \mathbf{P}] . \tag{10}$$

The solution is

$$\mathbf{P} = \frac{\epsilon_0}{4\pi}[\epsilon_0 \tilde{I} + (\tilde{\epsilon} - \epsilon_0 \tilde{I}) \cdot \tilde{L}]^{-1} \cdot (\tilde{\epsilon} - \epsilon_0 \tilde{I}) \cdot \mathbf{E}^{(e)} . \tag{11}$$

Equations (8) and (11) are equivalent.

The extinction cross section is[30]

$$C_E = \frac{V}{2S} \text{Re} \left[\mathbf{E}^{(e)*} \cdot \frac{d\mathbf{P}}{dt} \right]$$

$$= \frac{V\omega}{2S} \text{Im}(\mathbf{E}^{(e)*} \cdot \mathbf{P}) , \tag{12}$$

where $V = \frac{4}{3}\pi abc$ is the volume of the particle, $S = (\sqrt{\epsilon_0}c/8\pi)|\mathbf{E}^{(e)}|^2$ is the incident flux, and the asterisk denotes complex conjugation. Since the difference between extinction and absorption is negligible in the long-wavelength limit, the ED absorption coefficient is

$$\alpha_E = NC_E = \frac{f}{V} C_E . \tag{13}$$

N is the number density and f the volume fraction of particles embedded in the dielectric host. Interactions between the particles are neglected.

The results are

$$\alpha_E(\omega) = \frac{\sqrt{\epsilon_0}f\omega}{c}\text{Im}\{\hat{E}^{(e)*}\cdot(\overleftrightarrow{\epsilon}-\epsilon_0\overleftrightarrow{I})\cdot[\epsilon_0\overleftrightarrow{I}+\overleftrightarrow{L}\cdot(\overleftrightarrow{\epsilon}-\epsilon_0\overleftrightarrow{I})]^{-1}\cdot\hat{E}^{(e)}\} \qquad (14)$$

and

$$\alpha_E(\omega) = \frac{\sqrt{\epsilon_0}f\omega}{c}\text{Im}\{\hat{E}^{(e)*}\cdot[\epsilon_0\overleftrightarrow{I}+(\overleftrightarrow{\epsilon}-\epsilon_0\overleftrightarrow{I})\cdot\overleftrightarrow{L}]^{-1}\cdot(\overleftrightarrow{\epsilon}-\epsilon_0\overleftrightarrow{I})\cdot\hat{E}^{(e)}\} \qquad (15)$$

based on Eqs. (8) and (11), respectively. Here, $\hat{E}^{(e)}\equiv E^{(e)}/|E^{(e)}|$. Equation (14) has been obtained by Kononenko and Murzin.[32]

For spherical particles, Eqs. (14) and (15) reduce to[30]

$$\alpha_E(\omega) = \frac{9}{2}\sqrt{\epsilon_0}f\frac{\omega}{c}\text{Im}(\hat{E}^{(e)*}\cdot\overleftrightarrow{T}^{-1}\cdot\hat{E}^{(e)}) , \qquad (16)$$

where

$$\overleftrightarrow{T}\equiv\overleftrightarrow{I}+2\epsilon_0\overleftrightarrow{\epsilon}^{-1} . \qquad (17)$$

If the electromagnetic radiation is unpolarized, an average over polarizations must be performed. For propagation along the z axis,

$$\alpha_E(\omega) = \frac{9}{4}\sqrt{\epsilon_0}f\frac{\omega}{c}\text{Im}[T_{xx}^{-1}(\mathbf{H})+T_{yy}^{-1}(\mathbf{H})] . \qquad (18)$$

$\overleftrightarrow{T}(\mathbf{H})$ corresponds to a specific orientation of the anisotropic spherical particle. There is no simple expression for the average over orientations in the presence of a magnetic field. In zero field,

$$\alpha_E(\omega) = \frac{3}{2}\sqrt{\epsilon_0}f\frac{\omega}{c}\text{Im}[\text{Tr}(\overleftrightarrow{T}^{-1})] . \qquad (19)$$

2. Magnetic-dipole absorption

This discussion is based on work by Markiewicz[30] and by Visscher and Falicov.[33] The oscillating magnetic field of the incident wave induces an electric field according to Faraday's law. The induced eddy currents (Ohm's Law) produce a magnetic moment, which interacts with the oscillating magnetic field to produce energy absorption.

Faraday's law is

$$\nabla\times\mathbf{E} = \frac{i\omega}{c}\mathbf{B} , \qquad (20)$$

where $\mathbf{B}$ is the oscillating part of the magnetic field. The electric field is related to the induced current density by

$$\mathbf{E} = \overleftrightarrow{\rho}\cdot\mathbf{J} , \qquad (21)$$

where $\overleftrightarrow{\rho}$ is the resistivity tensor. Equations (20) and (21) are solved[33] by

$$\mathbf{J} = \mathbf{K}\times\mathbf{r} , \qquad (22)$$

where

$$\mathbf{K} = \frac{i\omega}{2c}\overleftrightarrow{\sigma}\cdot\mathbf{B} \qquad (23)$$

is a constant vector. $\overleftrightarrow{\sigma}\equiv\overleftrightarrow{\rho}^{-1}$ is an effective conductivity tensor, with

$$\overleftrightarrow{\rho}\equiv\frac{1}{2}[\text{Tr}(\overleftrightarrow{\rho})\overleftrightarrow{I}-\overleftrightarrow{\rho}^{\dagger}] . \qquad (24)$$

The dagger denotes the transpose.

The induced magnetic dipole moment is

$$\mathbf{M} = \frac{1}{2c}\int\mathbf{r}\times\mathbf{J}\,d\mathbf{r} . \qquad (25)$$

After integration,

$$\mathbf{M} = \frac{4\pi a^5}{15c}\mathbf{K} , \qquad (26)$$

where a is the radius of the spherical particle.

The rate of energy absorption is

$$P = \frac{1}{2}\text{Re}\left[\mathbf{B}^*\cdot\frac{d\mathbf{M}}{dt}\right]$$

$$= \frac{\omega}{2}\text{Im}(\mathbf{B}^*\cdot\mathbf{M}) . \qquad (27)$$

After substitution of Eq. (26),

$$P = \frac{\pi}{15}\frac{\omega^2 a^5}{c^2}\text{Re}(\mathbf{B}^*\cdot\overleftrightarrow{\sigma}\cdot\mathbf{B}) . \qquad (28)$$

The magnetic-dipole absorption coefficient is $\alpha_M=NP/S$, where $S=c|\mathbf{B}|^2/(8\pi\sqrt{\epsilon_0})$. Thus,

$$\alpha_M = \frac{2\pi}{5}\sqrt{\epsilon_0}fa^2\frac{\omega^2}{c^3}\text{Re}(\hat{B}^*\cdot\overleftrightarrow{\sigma}\cdot\hat{B}) , \qquad (29)$$

where $\hat{B}\equiv B/|B|$. Equation (29) is not consistent with the rigorous solution of FW,[28] but it should provide a good approximation when applied to small Bi particles. The average over polarizations, which is used in the calculations, is obtained by analogy with Eq. (18).

III. EXPERIMENT

A. Sample preparation and characterization

Bi particles were prepared by inert-gas evaporation.[34] The starting material was 99.999%-pure shot purchased from Aesar. The evaporations were performed in a diffusion-pumped system with a base pressure of 1×10^{-6} Torr.

Bi was placed in a tungsten boat. After pumping for about 30 min, 40 Torr of Linde research-grade, 99.9995%-pure Ar was let into the system. The particles were collected on the inside of a 3-l Pyrex beaker which was placed over the boat. Carbon-coated Cu grids were placed on the wall of the beaker to collect samples for electron microscopy. After the apparatus was allowed to cool, the vacuum was broken. The black powder was brushed from the beaker and stored in a vial for future use.

These particles, called sample A, were characterized by transmission electron microscopy (TEM). The volume-weighted mean diameter of the particles was 5000 Å. The micrographs show clusters of approximately spherical particles. Selected-area electron-diffraction patterns coincide with the rhombohedral structure of bulk Bi.

We also examine previously unpublished data of Chin and Sievers.[13] These particles, called sample B, were prepared by inert-gas evaporation in 100 mm of ^{4}He. The mean diameter was 4000 Å, as measured by TEM.

B. Far-infrared measurements

The spectroscopic studies were performed on samples of free-standing particles. There is evidence based on de Haas–van Alphen oscillations of the magnetic suscepti-bility[35] that unsupported Bi particles align with the bisec-trix axis parallel to the direction of the applied magnetic field. This alignment would be a great advantage when studying a highly anisotropic system. Although it is clear that the particles in the sample are touching, effects asso-ciated with individual particles are clearly observed and identified in our experiments. It is possible that oxide coatings isolate the particles electrically from one anoth-er.

Sample A was prepared by spreading a thin, uniform layer of the powder onto a Mylar sheet and sandwiching it with another layer of Mylar to keep the particles in place. Pinholes were made in the top Mylar sheet to al-low air to be pumped from the sample. For sample B, the powder was placed on a 1-mm-diam sapphire plate, which was wedged to eliminate channel oscillations due to multiple reflections.

Far-infrared magneto-optical studies were performed using Fourier-transform spectroscopy in the Faraday geometry. A field up to 7.5 T was provided by a super-conducting solenoid.[7] The samples were immersed in a ^{4}He bath ($T = 4.2$ K for sample B) which could be pumped ($T = 1.2$ K for sample A). Modulated FIR radi-ation was provided by a Michelson[36] (sample A) or lammelar-grating interferometer[37] (sample B). The radia-tion transmitted through the sample was detected by a pumped ^{3}He-cooled germanium bolometer.

IV. RESULTS AND DISCUSSION

The model described in Sec. II applies if the wave-length λ of the electromagnetic wave is much greater than the particle diameter d. Outside the particle, the re-lation $kd \ll 1$ with $k = 2\pi/\lambda$ is easily satisfied. The wavelength inside the particle is reduced so that $kd \lesssim 1$. Thus, the particles under consideration are not strongly in the quasistatic limit.

Figure 1 shows the frequency-dependent transmission ratio of the bismuth powder, sample A, for selected mag-netic fields. Each curve is the ratio of the transmission spectrum of the powder in the magnetic field to a zero-field spectrum. Magnetic-field-dependent resonances are clearly observed. The three strongest resonances are identified in the figure. These resonances were previously observed by Chin.[13] Each resonance becomes stronger as it moves up in frequency with increasing magnetic field.
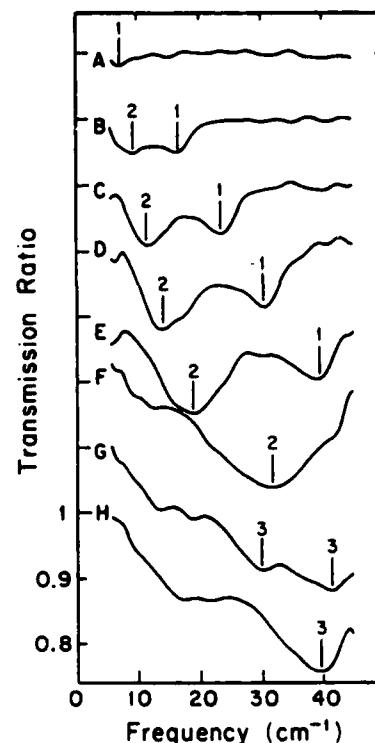

FIG. 1. Magnetic field dependence of the transmission ratio for unsupported small Bi particles. For each curve, the transmission spectrum at a chosen magnetic field is divided by a zero-field spectrum. The numbers indicate the strongest reso-nances. Additional resonances are observed in curves F, G, and H. The curves have been shifted for clarity. The magnetic fields (in T) are A—0.1, B—0.2, C—0.3, D—0.4, E—0.5, F—1.0, G—1.5, and H—2.0. The resolution is 2.2 cm^{-1}.
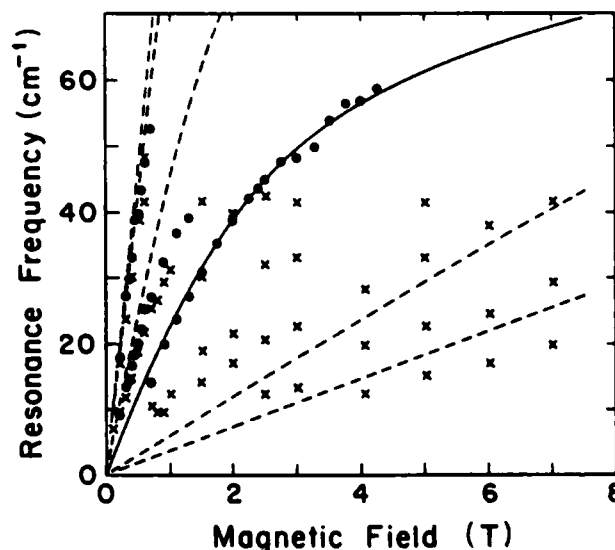

FIG. 2. Magnetic field dependence of cyclotronlike hybrid resonance frequencies in Bi powders. X's indicate data on sam-ple A, and circles, sample B. The solid and dashed lines show the electric- and magnetic-dipole resonances, respectively, pre-dicted by the model with the binary axis of the particles aligned along the applied magnetic field.
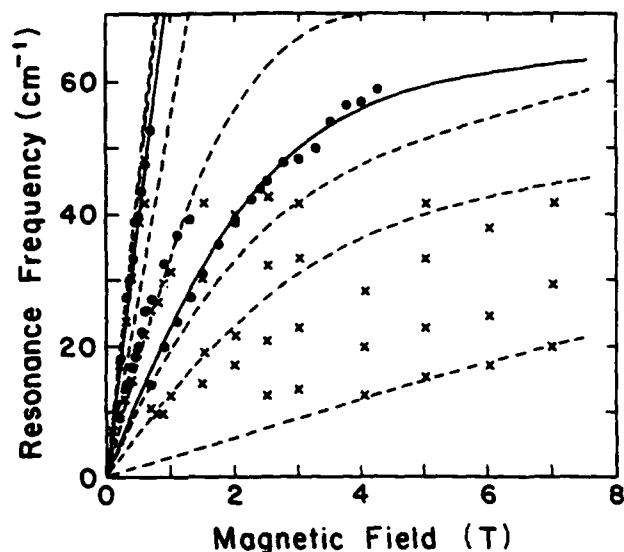
FIG. 3. Magnetic field dependence of resonance frequencies in Bi powders. X's indicate data on sample A, and circles, sample B. The solid and dashed lines show the electric- and magnetic-dipole resonances, respectively, predicted by the model with the bisectrix axis of the particles aligned along the magnetic field.
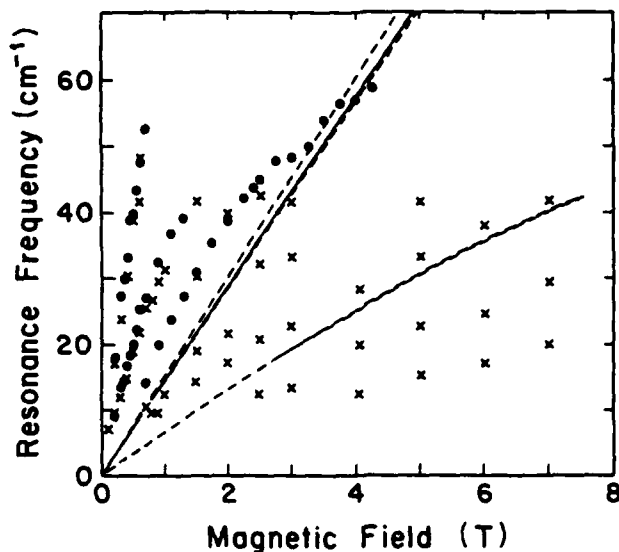
FIG. 4. Magnetic field dependence of resonance frequencies in Bi powders. X's indicate data on sample A, and circles, sample B. The solid and dashed lines show the electric- and magnetic-dipole resonances, respectively, predicted by the model with the trigonal axis of the particles aligned along the magnetic field.

There is clear evidence for additional resonances in the data. The transmission data at higher fields show additional new resonances. It is remarkable that these resonances, which are associated with single-particle behavior, are observed in powder samples for which the particles are clearly in contact. Since Bi forms an oxide, the particles are almost certainly oxide coated.

Figure 2, as well as Figs. 3 and 4, shows the magnetic field dependence of the observed resonance frequencies for sample A. Also shown are the data of Chin and Sievers,[13] which confirm our measurements for the strongest resonances and extend them to higher frequencies. All of the observed resonances are cyclotronlike in the sense that the resonance frequency vanishes as the magnetic field approaches zero. They are hybrid resonances because they are not, in general, associated with the motion

TABLE I. Calculated absorption strengths for magnetic-field-induced resonances in small Bi particles.

Crystallographic axis parallel to H	Resonance type	$\bar{\omega}=20$ cm^{-1}		$\bar{\omega}=40$ cm^{-1}	
		H (T)	α (cm^{-1})	H (T)	α (cm^{-1})
Binary axis	ED	0.882	0.558	2.080	9.690
	MD	0.217	0.160	0.433	0.560
	MD	0.238	0.038	0.479	0.148
	MD	0.411	0.239	0.864	0.942
	MD	3.371	0.177	6.900	0.732
	MD	5.453	0.111	11.105	0.493
Bisectrix axis	ED	0.256	0.036	0.517	0.686
	ED	0.875	0.006	2.032	0.114
	MD	0.221	0.150	0.444	0.571
	MD	0.231	0.003	0.466	0.006
	MD	0.373	0.314	0.746	1.252
	MD	0.584	0.111	1.249	0.417
	MD	1.057	0.004	2.757	0.011
	MD	1.688	0.080	5.046	0.251
	MD	7.071	0.069	19.621	0.312
Trigonal axis	ED	1.394	0.0006	2.788	0.009
	MD	1.326	0.533	2.652	2.127
	MD	1.410	0.051	2.820	0.194
	MD	3.134	0.117	6.958	0.491
	MD	3.154	0.118	7.007	0.494

of a single type of charge carrier. The effective masses estimated from the zero-field slopes [using $\omega = eH/(m^*c)$] do not correlate in a simple way with the known effective masses for bulk Bi. Also, such a large number of resonances is surprising. Curvature is observed in the dependence of the resonance frequency on applied field. Curvature observed in cyclotron resonances for bulk Bi is associated with band nonparabolicity.[17] The bending observed here is associated with the interaction of the cyclotronlike hybrid modes with the sphere plasma resonances. Clearly, the size and shape of the particles contribute to the determination of the resonance frequencies.

Figures 2–4 also show the calculated field dependence of the resonance frequencies for Bi particles in the Faraday geometry with binary, bisectrix, and trigonal orientations, respectively. For example, in Fig. 2 the particles are oriented with the applied magnetic field and the direction of propagation of the FIR radiation along the binary axis. No parameters were adjusted to fit the calculated resonance frequencies with the data.

The complexity of the Bi dielectric tensor arising from both the multiplicity of carriers and their anisotropy rules out a simple search for resonance frequencies by locating the zeros of polynomials in the denominators of expressions for the absorption coefficient. Instead, the following method was used: A small relaxation rate was chosen [$(2\pi c\tau)^{-1} = 0.1$ cm^{-1}]. Resonances were located by examining the frequency dependence of the calculated absorption coefficient to a resolution of 0.1 cm^{-1}. There is the possibility in this method of missing resonances, particularly weak ones, or not resolving resonances that are nearly degenerate. There is also the possibility of experimentally observing additional resonances not allowed in the calculations, which are based strictly on the Faraday geometry. None of these details are relevant to the interpretation of the data.

Table I lists the calculated resonance magnetic fields and absorption coefficients for two selected frequencies within the experimentally accessible range. The resonance field is accurate to 0.001 T, and $1/(2\pi c\tau) = 0.1$ cm^{-1} was used. The particle radius is $a = 2500$ Å, the host is vacuum ($\epsilon_0 = 1$), and the volume fraction of Bi is $f = 0.01$. The values for α are for relative comparison. The absolute magnitudes mean little. Magnetic-dipole absorption depends explicitly on a^2 relative to electric-dipole absorption, and hence is relatively stronger for larger particles.

All three orientations are required to explain the number of observed resonances. There is no convincing evidence to support alignment of the particles along the bisectrix direction. Both electric- and magnetic-dipole resonances are observed. The observation of magnetic-dipole resonances is especially interesting, because reports of their observation in very small particles are rare.[38] Magnetic-dipole absorption dominates in larger electron-hole droplets,[30] but in this case the theoretical description based on the long-wavelength limit is inadequate. The ED and MD resonances identified by comparison of the data with the model are of comparable strength. The model predicts that a resonance grows in strength with increasing magnetic field (Table I), in agreement with the data.

All ED resonances predicted by the model are identified in the data, and the agreement is excellent. The resonance identified as 3 in Fig. 1 is associated with ED absorption of binary and/or bisectrix oriented particles. According to Table I, the resonance for binary oriented particles is the stronger. The weakest ED resonance according to the model, associated with the trigonal alignment, is also the least convincingly identified in the data.

The remaining resonances must be magnetic dipole. The detailed agreement between theory and experiment for MD resonances is not as good as for ED resonances, but the theory is not rigorously correct. Also, the particles are a bit large for the quasistatic limit to strongly apply. Based on the calculated absorption strengths, resonance 1 is predominantly MD, although it is also consistent with ED absorption. Resonance 2 is clearly MD. However, the model predicts a stronger MD resonance between resonances 1 and 2. The data (Fig. 1) show evidence for such a resonance, but it is weak. With the exception of the lowest MD resonance for the bisectrix orientation, the low-frequency MD resonances are not well matched by the model. However, there is agreement between the numbers of predicted and observed resonances if it is noted that two of the trigonal resonances are essentially degenerate with a binary MD resonance.

While the analysis based on three orientations leads to a clear interpretation, it is oversimplified. For an ensemble of randomly oriented Bi particles in a magnetic field, each orientation corresponds to a unique system with its own set of resonance frequencies. Unlike the $H = 0$ case [Eq. (19)], the ensemble average cannot be written as the trace of a single matrix. Preliminary results based on Monte Carlo calculations support the principal conclusions of the simplified analysis. For example, the resonances observed below 40 cm^{-1} at the highest fields must be MD.

V. CONCLUSIONS

Observed magnetic-field-dependent far-infrared resonances in submicrometer free-standing Bi particles in the form of a smoke are successfully described by a model for isolated particles based on the quasistatic approximation. The model makes use of the experimentally determined parameters of bulk Bi. Both electric- and magnetic-dipole resonances are observed. We conclude that these particles are bulklike in nature.

There are a number of directions in which the study of Bi particles can be extended. The particles can be embedded in a supporting nonabsorbing host to better isolate them from one another. With a more dilute sample, magneto-optical studies can be extended to include the frequency region of the sphere plasma resonance[39] (~ 170 cm^{-1}). Such data would further test the model. Particles with smaller mean sizes should also be examined to determine the limitations of a description based on bulk properties and to identify any new effects that may occur, such as a possible size-induced semimetal-semiconductor transition. Such studies are underway in our laboratory.

ACKNOWLEDGMENTS

[1] V. S. Edel'man, Adv. Phys. 25, 555 (1976).

[2] L. A. Fal'kovskii, Usp. Fiz. Nauk 94, 3 (1968) [Sov. Phys.—Usp. 11, 1 (1968)].

[3] W. S. Boyle and G. E. Smith, in Progress in Semiconductors, edited by A. F. Gibson and R. E. Burgess (Wiley, New York, 1963), Vol. 7, p. 1.

[4] W. S. Boyle and A. D. Brailsford, Phys. Rev. 120, 1943 (1960).

[5] L. C. Hebel and P. A. Wolff, Phys. Rev. Lett. 11, 368 (1963).

[6] J. C. Burgiel and L. C. Hebel, Phys. Rev. 140, A925 (1965).

[7] R. L. Blewitt and A. J. Sievers, J. Low Temp. Phys. 13, 617 (1973).

[8] V. D. Kulakovskii, V. V. Rozhdestvenskaya, A. G. Belov, V. S. Vavilov, A. A. Gippina, V. D. Egorov, and V. S. Zemskov, Fiz. Tekh. Poluprovdn. 6, 2268 (1972) [Sov. Phys.—Semicond. 6, 1912 (1973)].

[9] H. D. Drew and U. Strom, Phys. Rev. Lett. 25, 1755 (1970).

[10] U. Strom, H. D. Drew, and J. F. Koch, Phys. Rev. Lett. 26, 1110 (1971).

[11] U. Strom, A. Kamgar, and J. F. Koch, Phys. Rev. B 7, 2435 (1973).

[12] H. R. Verdun and H. D. Drew, Phys. Rev. B 14, 1370 (1976); H. D. Drew and H. R. Verdun, Phys. Condensed Matter 19, 371 (1975).

[13] A. K. Chin, Ph.D. thesis, Cornell University, Ithaca, NY, 1977.

[14] B. Lax, J. G. Mavroides, H. J. Zeiger, and R. J. Keyes, Phys. Rev. Lett. 5, 241 (1960).

[15] R. N. Brown, J. G. Mavroides, M. S. Dresselhaus, and B. Lax, Phys. Rev. Lett. 5, 243 (1960).

[16] R. N. Brown, J. G. Mavroides, and B. Lax, Phys. Rev. 129, 2055 (1963).

[17] M. Maltz and M. S. Dresselhaus, Phys. Rev. B 2, 2877 (1970).

[18] M. P. Vecchi and M. S. Dresselhaus, Phys. Rev. B 9, 3257 (1974).

[19] M. P. Vecchi and M. S. Dresselhaus, Phys. Rev. B 10, 771 (1974).

[20] M. P. Vecchi, J. R. Pereira, and M. S. Dresselhaus, Phys. Rev. B 14, 298 (1976).

[21] R. P. Devaty, Phys. Rev. B 38, 7972 (1988), and references therein.

[22] F. L. Galeener and J. K. Furdyna, Phys. Rev. B 4, 1853 (1971); T. A. Evans and J. K. Furdyna, ibid. 8, 1461 (1973).

[23] J. R. Dixon, Jr. and J. K. Furdyna, Phys. Rev. B 18, 6770 (1978).

[24] R. S. Markiewicz and T. Timusk, in Electron-Hole Droplets in Semiconductors, edited by C. D. Jeffries and L. V. Keldysh (North-Holland, New York, 1983), pp. 543–618.

[25] B. Lax, K. J. Button, H. J. Zeiger, and L. M. Roth, Phys. Rev. 102, 715 (1956).

[26] B. Lax and J. G. Mavroides, in Solid State Physics, edited by F. Seitz and D. Turnbull (Academic, New York, 1960), Vol. 11, p. 261.

[27] S. Takano and H. Kawamura, J. Phys. Soc. Jpn. 28, 348 (1970).

[28] G. W. Ford and S. A. Werner, Phys. Rev. B 18, 6752 (1978).

[29] G. Mie, Ann. Phys. (Leipzig) [Folge 4] 25, 377 (1908).

[30] R. S. Markiewicz, Phys. Rev. B 18, 4260 (1978).

[31] L. D. Landau and E. M. Lifshitz, Electrodynamics of Continuous Media (Pergamon, Oxford, 1960), pp. 20–27 and 42–45.

[32] V. L. Kononenko and V. N. Murzin, Zh. Eksp. Teor. Fiz. 75, 124 (1978) [Sov. Phys.—JETP 48, 61 (1978)].

[33] P. B. Visscher and L. M. Falicov, Phys. Rev. B 2, 1518 (1970).

[34] C. G. Granqvist and R. A. Buhrman, J. Appl. Phys. 47, 2200 (1976).

[35] J. Feder and D. S. McLachlan, Phys. Lett. 29A, 431 (1969).

[36] K. C. Johnson, Ph.D. thesis, Cornell University, Ithaca, NY, 1972.

[37] I. G. Nolt, R. D. Kirby, C. D. Lytle, and A. J. Sievers, Appl. Opt. 8, 309 (1969).

[38] V. I. Gavrilenko, V. L. Kononenko, T. S. Mandel'shtam, V. N. Murzin, and S. A. Saunin, Pis'ma Zh. Eksp. Teor. Fiz. 26, 102 (1977) [JETP Lett. 26, 95 (1977)].

[39] R. E. Sherriff and R. P. Devaty, Bull. Am. Phys. Soc. 33, 282 (1988).